

Serotonin Reciprocally Regulates Melanocortin Neurons to Modulate Food Intake

Lora K. Heisler,^{1,2,12} Erin E. Jobst,^{3,4}
Gregory M. Sutton,⁵ Ligang Zhou,¹ Erzsebet Borok,⁶
Zoe Thornton-Jones,⁷ Hong Yan Liu,⁸
Jeffrey M. Zigman,² Nina Balthasar,² Toshiro Kishi,⁹
Charlotte E. Lee,² Carl J. Aschkenasi,²
Chen-Yu Zhang,² Jia Yu,² Olivier Boss,²
Kathleen G. Mountjoy,¹⁰ Peter G. Clifton,⁷
Bradford B. Lowell,² Jeffrey M. Friedman,⁸
Tamas Horvath,⁶ Andrew A. Butler,⁵
Joel K. Elmquist,^{2,11,*} and Michael A. Cowley^{3,*}

¹Department of Clinical Biochemistry
Addenbrooke's Hospital
University of Cambridge
Cambridge, CB2 2QQ
United Kingdom

²Division of Endocrinology, Diabetes and Metabolism
Departments of Medicine and Neurology
Beth Israel Deaconess Medical Center and
Program in Neuroscience
Harvard Medical School
Boston, Massachusetts 02215

³Division of Neuroscience
Oregon National Primate Research Center
Oregon Health and Science University
Beaverton, Oregon 97006

⁴School of Physical Therapy
Pacific University
Forest Grove, Oregon 97116

⁵Pennington Biomedical Research Center
Louisiana State University System
Baton Rouge, Louisiana 70808

⁶Department of Obstetrics and Gynecology and the
Department of Neurobiology
Yale Medical School
New Haven, Connecticut 06520

⁷Department of Psychology
Sussex University
Brighton BN1 9QG
United Kingdom

⁸Laboratory of Molecular Genetics
Howard Hughes Medical Institute
The Rockefeller University
New York, New York 10021

⁹Department of Anatomy and Morphological
Neuroscience
Shimane University School of Medicine
Izumo 693-8501
Japan

¹⁰Department of Physiology
Faculty of Medical and Health Science
University of Auckland
New Zealand

¹¹Department of Internal Medicine
University of Texas Southwestern Medical Center
Dallas, Texas 75390

*Correspondence: joel.elmquist@UTSouthwestern.edu (J.K.E.);
cowleym@ohsu.edu (M.A.C.)

¹²Additional correspondence: lkh30@medschl.cam.ac.uk (L.K.H.)

Summary

The neural pathways through which central serotonergic systems regulate food intake and body weight remain to be fully elucidated. We report that serotonin, via action at serotonin_{1B} receptors (5-HT_{1B}Rs), modulates the endogenous release of both agonists and antagonists of the melanocortin receptors, which are a core component of the central circuitry controlling body weight homeostasis. We also show that serotonin-induced hypophagia requires downstream activation of melanocortin 4, but not melanocortin 3, receptors. These results identify a primary mechanism underlying the serotonergic regulation of energy balance and provide an example of a centrally derived signal that reciprocally regulates melanocortin receptor agonists and antagonists in a similar manner to peripheral adiposity signals.

Introduction

Serotonin (5-hydroxytryptamine, 5-HT) analogs have been widely developed as weight-loss agents, based largely on early observations of the strong inverse relationship between 5-HT levels and food consumption (Breisch et al., 1976; Garattini et al., 1986; Goudie et al., 1976; Samanin et al., 1980). 5-HT does not cross the blood-brain barrier, and it is synthesized in both the periphery and brain from the essential amino acid tryptophan. It is speculated that 5-HT-induced appetite suppression is predominantly mediated by central 5-HT pathways, although the mechanism has not been fully defined. It is well established that within the brain the arcuate nucleus of the hypothalamus (ARC) plays an important role in energy homeostasis (Cone, 2005; Elmquist et al., 1999; Gropp et al., 2005; Luquet et al., 2005) and is thus a strong candidate to function as a central nucleus subserving 5-HT-induced hypophagia.

The ARC contains two distinct populations of neurons: one expressing the endogenous anorectic melanocortin receptor agonist, α -melanocyte stimulating hormone (α -MSH), and the other expressing the endogenous orexigenic melanocortin receptor antagonist, agouti-related protein (AgRP) (Elias et al., 1998; Hahn et al., 1998; Broberger et al., 1998). Both α -MSH and AgRP are potent modulators of food intake and body weight and are reciprocally regulated by peripheral signals, such as the adipose tissue-derived hormone leptin and the gastrointestinal hormone ghrelin (Ahima et al., 1999; Cowley et al., 2003; Elias et al., 1999). We hypothesize that melanocortin pathways are also differently regulated by centrally derived signals, such as 5-HT, and that melanocortin circuitry is a primary mechanism underlying 5-HT's effects on energy balance. Consistent with this hypothesis, the 5-HT reuptake inhibitor/5-HT stimulated release compound d-fenfluramine and 5-HT_{2C}R agonists activate α -MSH-containing neurons (Heisler et al., 2002). However, it is not known whether 5-HT pathways, in concert, regulate the signaling of AgRP-containing neurons, the mechanism of this prospective regulation, or

downstream melanocortin receptor targets mediating 5-HT-induced hypophagia.

A 5-HT receptor that is positioned to affect ARC AgRP activity is the 5-HT_{1B}R (rodent homolog to human 5-HT_{1Dβ}R) (Bruinvels et al., 1994; Makarenko et al., 2002). This receptor has been strongly implicated in 5-HT-induced hypophagia. Specifically, high-affinity 5-HT_{1B}R agonists produce substantial reductions in food intake, effects that are attenuated by pharmacological blockade or genetic inactivation of 5-HT_{1B}Rs (Halford and Blundell, 1996; Lee et al., 1998; Lee and Simansky, 1997; Lucas et al., 1998). 5-HT_{1B}Rs are G_i-coupled to inhibit adenylate cyclase and are expressed on 5-HT presynaptic terminals and postsynaptic terminals. 5-HT_{1B}Rs are also expressed on nonserotonergic presynaptic terminals where they regulate the release of other neurotransmitters, such as γ -amino butyric acid (GABA) (Chadha et al., 2000; Stanford and Lacey, 1996). We hypothesize that 5-HT_{1B}Rs are expressed both on AgRP-containing neurons and on the AgRP inhibitory axonal projections to POMC-containing neurons (Cowley et al., 2001, 2003; Roseberry et al., 2004). If this is the case, then 5-HT action at ARC 5-HT_{1B}Rs would lead to a decrease in the release of the endogenous melanocortin receptor (MCR) antagonist and an increase in the release of the endogenous MCR agonist at downstream MCR-expressing target sites.

Within the brain, α -MSH and AgRP compete for action at Mc3rs and Mc4rs (Cone, 2005). Of these receptors, the Mc4rs have been demonstrated to produce the most potent effects on food intake, body weight, energy expenditure, and insulin action (Fan et al., 2000; Huszar et al., 1997). In fact, dysregulation of Mc4rs is associated with the most common monogenic cause of human obesity identified thus far (Farooqi et al., 2000; Vaisse et al., 1998). Consistent with this finding, Mc4rs are expressed in multiple central regions associated with energy homeostasis, such as the paraventricular nucleus of the hypothalamus and the dorsal motor nucleus of the vagus (Kishi et al., 2003; Liu et al., 2003; Mountjoy et al., 1994). If 5-HT requires melanocortin pathways to regulate energy balance, then downstream action at the Mc4rs is a likely downstream component of this circuitry.

In the present study, we examined whether 5-HT pathways are anatomically positioned to differently regulate the signaling of central melanocortin agonist- and antagonist-containing neurons. We assessed whether this regulation is achieved via action at the 5-HT_{1B}R, the only G_i-coupled 5-HT receptor associated with satiety known to be expressed in the ARC that acts as both a postsynaptic receptor and heteroreceptor. Finally, we determined whether Mc4rs are a necessary downstream target of 5-HT agonist-induced hypophagia. The findings presented here further define the pathways underlying 5-HT's effects on energy homeostasis, a neurotransmitter system that has been a major target for obesity treatment.

Results

5-HT_{1B}Rs Are Expressed in NPY/AgRP-Containing Neurons

Transgenic mice expressing tau-sapphire green fluorescent fusion protein (GFP) under the control of a NPY

promoter/enhancer were used to identify ARC cells expressing NPY/AgRP for anatomical and physiological studies (NPY-GFP mice) (Cowley et al., 2003; Pinto et al., 2004; Roseberry et al., 2004). We confirmed that GFP is exclusively expressed in AgRP mRNA-containing neurons (99.5%) throughout the rostral caudal extent of the ARC in NPY-GFP mice using *in situ* hybridization histochemistry (ISHH) with a ³⁵S-labeled riboprobe for AgRP mRNA coupled with immunohistochemistry (IHC) for GFP (GFP-IR) (n = 5; Figures 1A and 1B). These data indicate that ARC cells expressing GFP contain AgRP mRNA.

Next, by generating a 5-HT_{1B}R riboprobe that identified 5-HT_{1B}R mRNA in mice with ISHH, we investigated whether 5-HT_{1B}Rs are positioned to affect AgRP activity. Consistent with earlier reports in rats (Bonaventure et al., 1998; Bruinvels et al., 1994), we observed that 5-HT_{1B}R mRNA is abundantly expressed in the wild-type mouse brain, with particularly high levels in the olfactory tubercle, caudate putamen, cortex, hypothalamus (including the ARC; Figure 1C), hippocampal formation, thalamus, dorsal raphe, and cerebellum (n = 5). Using double labeling for ³⁵S-5-HT_{1B}R and GFP-IR in NPY-GFP mice, we determined that approximately one-third of ARC 5-HT_{1B}R-expressing neurons were GFP-IR positive and that one-sixth of ARC GFP-IR neurons were 5-HT_{1B}R positive (n = 3; Figure 1D). These findings indicate that 5-HT_{1B}Rs are anatomically positioned to affect the activity of a subpopulation of ARC AgRP neurons.

5-HT Terminals Are in Close Apposition to NPY/AgRP Neurons

We performed light and electron microscopic analysis to determine whether 5-HT terminals establish synaptic contacts with AgRP-containing neurons. Using dual-label IHC in brain tissue from NPY-GFP mice, we found that 5-HT boutons are in direct apposition both to ARC GFP cell bodies and to proximal and distal dendrites (n = 3–5; Figures 1E–1H). Specifically, we observed that approximately one-third (mean \pm SEM, 34 \pm 5, out of 100) of GFP-positive profiles were contacted by 5-HT-IR putative axon terminals in NPY-GFP mice. Electron microscopic analysis confirmed that 5-HT axon terminals established synapses on these neurons (Figures 1I and 1J). Additionally, close proximity of 5-HT and GFP boutons was noted presynaptic to unidentified ARC perikarya (Figure 1E). These observations suggest that 5-HT may produce a dual effect on AgRP neurons, affecting both neuronal activity and the release of products from the axon.

Effect of 5-HT and 5-HT_{1B}R Agonists on Activity of NPY/AgRP and α -MSH Neurons

We used an electrophysiological approach to establish the functional relevance of our anatomical observations. Using GFP-labeled cells in ARC slices of NPY-GFP mouse brains, we observed a trend of bath-applied 5-HT (30 μ M) hyperpolarization of GFP neurons [8.1 \pm 7.1 mV, n = 3, t(2) = 1.99, n.s.; Figure 2A], and this effect was reversible with 5-HT washout. These findings suggest that 5-HT likely reduces the release of AgRP at downstream central sites. Consistent with mediation of 5-HT action at 5-HT_{1B}Rs, selective 5-HT_{1B}R agonists hyperpolarized NPY-GFP neurons (Figure 2A). Specifically,

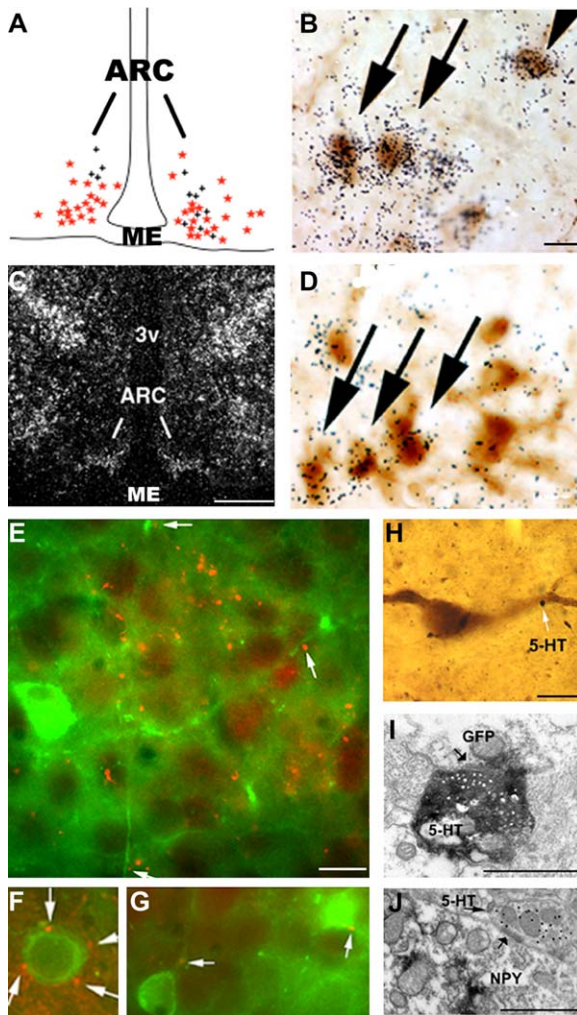


Figure 1. NPY/AgRP-Containing ARC Neurons Coexpress 5-HT_{1B}R and Display Close Apposition to 5-HT Axon Terminals

(A) Schematic of representative level of the ARC illustrating that 99.5% of neurons containing GFP-IR colocalized with ³⁵S-labeled AgRP (red stars) in mice expressing tau-sapphire green fluorescent fusion protein under the control of a NPY promoter (NPY-GFP). Some neurons were only labeled by ³⁵S-AgRP (black pluses). (B) Representative photograph illustrating neurons containing GFP-IR (brown cytoplasm) colocalized with ³⁵S-labeled AgRP (cluster of black grains) in the ARC of NPY-GFP mice. (C) Neurons containing ³⁵S-labeled 5-HT_{1B}R (white grains) under darkfield illumination are expressed in the ARC as determined with ISSH in wild-type mice (n = 5). (D) Dual-labeling for IHC and ISSH revealed that ARC neurons expressing GFP-IR (brown cytoplasm) colocalized with ³⁵S-labeled 5-HT_{1B}R (black grains) in NPY-GFP mice (n = 3). Using dual fluorescence for GFP (green profiles) and 5-HT (red profiles), both putative axodendritic ([E and G], white arrows) and axosomatic ([F and G], white arrows) contacts between 5-HT-IR boutons and GFP-NPY cells in the ARC were revealed. (H) Dual-IHC labeling further illustrated that proximal dendrites from GFP-IR cells (brown reaction product) were in close proximity to 5-HT-IR boutons (black reaction product). (I) Correlated electron microscopy demonstrated that this is a direct connection, indicating synaptic interaction (wide black arrow) between this 5-HT bouton and the GFP dendrite. (J) In further clarifying that these membrane specializations are indeed synaptic in nature, postembedding labeling of 5-HT using 5 nm gold-conjugated secondary antisera showed clear synaptic membrane specialization (wide black arrow) between a 5-HT-immunopositive bouton (narrow black arrow) and the perikaryal membrane of a GFP neuron in the ARC. Scale bar represents 20 μm in (B) and also applies to (D),

the selective 5-HT_{1B}R agonists CP94253 [200 nM, n = 5, t(4) = 3.52, p < 0.05] and CP93129 [200 nM, n = 3, t(2) = 3.20, p < 0.09] hyperpolarized the membrane potential of identified GFP neurons (10 of 14 assessed; Figures 2A and 2B). In the GFP-NPY neurons that were spontaneously firing action potentials (7 of 10 GFP neurons tested), 5-HT_{1B}R agonists hyperpolarized 6 of these 7 neurons with an accompanying 78% ± 9% decrease in spontaneous firing frequency. The selective 5-HT_{1B}R antagonist SB224289 (200 nM) prevented significant hyperpolarization induced by CP94253 (200 nM) alone, resulting in a net change in membrane potential of 0.65 ± 1.0 mV (n = 4; Figure 2A). These data suggest that 5-HT reduces AgRP neuron activity via action at 5-HT_{1B}R.

A strong inhibitory GABAergic projection exists between NPY/AgRP neurons and proopiomelanocortin (POMC, the uncleaved precursor of α-MSH) cells in the ARC (Cowley et al., 2001; Roseberry et al., 2004). Because 5-HT_{1B}Rs are expressed on nonserotonergic axon terminals and have been demonstrated to affect GABA release in other brain regions (Chadha et al., 2000; Stanford and Lacey, 1996), we hypothesized that 5-HT may also affect POMC activity via 5-HT_{1B}R expressed on inhibitory NPY/AgRP terminals projecting to POMC neurons in the ARC. To examine this, we exploited transgenic mice expressing GFP under the transcriptional control of the POMC gene promoter. We measured inhibitory postsynaptic currents (IPSCs) onto GFP neurons in hypothalamic slices from POMC-GFP mice (Cowley et al., 2001). 5-HT [30 μM, n = 6, t(5) = 6.98, p < 0.05] and 5-HT_{1B}R agonists CP94253 [100 nM, n = 5, t(4) = 2.84, p < 0.05] and CP93129 [100 nM, n = 12, t(11) = 11.08, p < 0.05] reversibly reduced IPSCs in GFP-labeled POMC neurons by approximately one-third (Figures 2C–2F). Of note, the effect of CP94253 and CP93129 on IPSC frequency onto POMC neurons was seen at a lower drug concentration than the effect on NPY/AgRP neuron membrane potential. This is likely due to technological issues related to the difficulty of reliably quantifying small changes in membrane potential, whereas small changes in IPSC frequency can be more reliably assessed. Taken together, the results presented here indicate that 5-HT, via action at 5-HT_{1B}R, both reduces the likelihood of release of AgRP and facilitates the release of α-MSH at downstream target sites.

Melanocortin Pathways Are Required for 5-HT Probes to Promote Satiety

We next assessed the effect of the 5-HT indirect agonist and antiobesity compound d-fenfluramine (d-fen) in mice with constitutive ectopic expression of the endogenous MCR antagonist, agouti peptide (Ay mice). It is well established that 5-HT probes may suppress food intake by either advancing satiety or by interfering with food intake (e.g., by enhancing sedation), since 5-HT modulates a wide variety of behaviors and physiological processes. For example, Vickers and colleagues demonstrated that 3.0 mg/kg of d-fen specifically

250 μm in (C); scale bar in (E) and (H) represents 10 μm and also applies to (F) and (G); scale bar represents 1 μm in (I) and (J). 3v, third ventricle; ME, median eminence, ARC, arcuate nucleus of the hypothalamus; 5-HT, serotonin; GFP, green fluorescent protein.

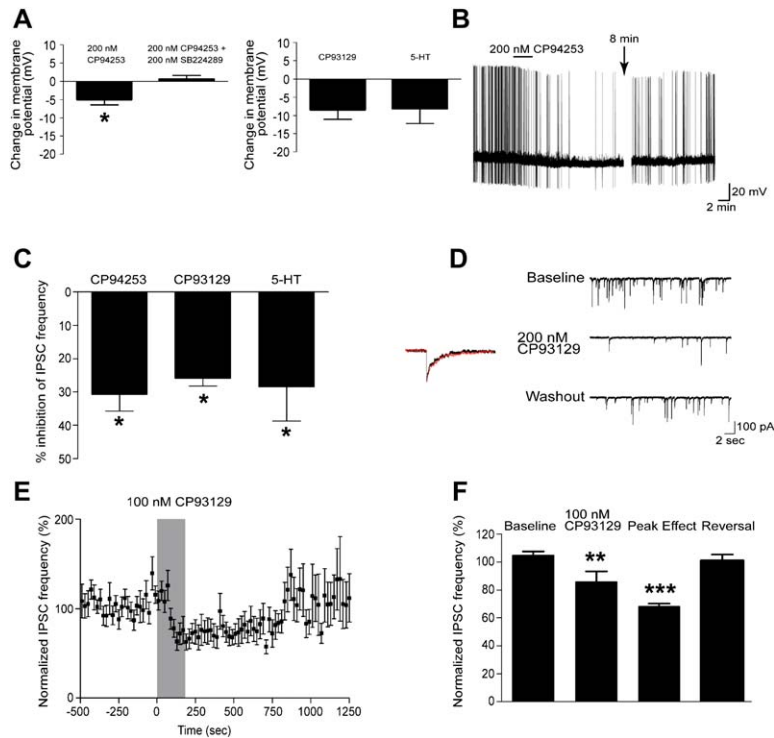


Figure 2. 5-HT and 5-HT_{1B}R Agonists Hyperpolarize ARC NPY/AGRP Neurons and Decrease Inhibitory Synaptic Input onto POMC Neurons

(A) Bath application of CP94253 (200 nM; n = 6) significantly hyperpolarized ARC GFP-NPY neurons; the effect was blocked by coapplication with the selective 5-HT_{1B}R antagonist SB224289 (200 nM; n = 4). CP93129 (200 nM; n = 3) and 5-HT (30 μM; n = 3) also hyperpolarized ARC NPY neurons. Data are expressed as mean ± SEM.

(B) Example of raw data showing that CP94253 (200 nM) hyperpolarized and decreased the spontaneous activity of a single ARC NPY neuron. Mean of membrane potential 5 min prior to agonist application = -51.4 mV; during agonist application (3.2 min) = -53.7 mV; peak effect 9 min into washout = -57.7 mV; recovery 30 min into washout = -52.8 mV. Firing frequency prior to agonist application = 0.2 Hz; during agonist = 0.15 Hz; during peak hyperpolarization = 0.007 Hz; during partial recovery = 0.05 Hz.

(C) CP94253 (100 nM; n = 5), CP93129 (100 nM; n = 12), and 5-HT (30 μM; n = 6) significantly decreased the frequency of spontaneous IPSCs onto ARC POMC neurons. Data are expressed as mean ± SEM.

(D) Examples of raw data showing IPSCs before, during, and after bath application of 200 nM CP93129. Inset demonstrates representative kinetics of GABA-induced ionic conductances superimposed at a higher magnification (peak current is 65 pA in 400 ms window) before agonist application (black) and during peak effect (red).

(E) CP93129 (100 nM) reversibly decreases the inhibitory synaptic input onto POMC neurons (n = 12). Shaded region corresponds to time of drug application. Data are expressed as mean ± SEM.

(F) Cumulative frequency histogram demonstrating the reversible effect of CP93129 (100 nM) on IPSC frequency onto ARC POMC neurons [Baseline versus CP93129 t(34) = 3.14, p < 0.01; Baseline versus Peak Effect t(55) = 11.77, p < 0.001; Baseline versus Reversal t(46) = 0.81, n.s.]. *p < 0.05, **p < 0.01, ***p < 0.001 (compared to baseline or hypothesized 0). Data are expressed as mean ± SEM.

reduced food intake by advancing the behavioral satiety sequence, whereas higher doses (e.g., 10–30 mg/kg) induced behaviors like stereotypy that disrupt feeding (Vickers et al., 1999). Lee and colleagues also reported that higher concentrations of d-fen (5.6–30 mg/kg) interrupt normal feeding-behavior patterns in wild-type mice (Lee et al., 2004).

To investigate the role of melanocortin pathways selectively in 5-HT-induced satiety, we treated young lean male *Ay* mice and weight-matched wild-type littermates (n = 10 per genotype) with a low dose of d-fen (1.5 mg/kg, i.p.), a dose that advances satiety (3.0 mg/kg, i.p.), and a dose that enhances resting/inactive behavior (6.0 mg/kg, i.p.). D-fen significantly reduced 1 hr chow mash intake at the onset of the dark cycle in wild-type mice [F(3,18) = 3.91, p < 0.05, post hoc saline versus d-fen 3.0 and 6.0 mg/kg; Figure 3A]. In contrast, *Ay* littermates did not alter 1 hr chow mash intake following any dose of d-fen except that which promotes resting and consequently disrupts feeding [F(3,18) = 3.79, p < 0.05, post hoc d-fen 6.0 mg/kg versus all other doses; Figure 3B]. The induction of behaviors that compete with feeding at higher concentrations of 5-HT probes is likely associated with the lack of 5-HT receptor selectivity, which confounds the interpretation of the specific pathways modulating 5-HT's effects on satiety.

We therefore investigated the mechanism of 5-HT-induced satiety via action at the 5-HT_{1B}Rs using the

selective 5-HT_{1B}R agonist CP94253 (K_i 5-HT_{1B}R = 2, 5-HT_{1A}R = 89, 5-HT_{2C}R = 860, 5-HT_{1D}R = 49, and 5-HT_{2A}R = 1600 nM; Koe et al., 1992). This compound enhances satiety and produces a behavioral profile comparable to prefeeding in rodents (Halford and Blundell, 1996; Lee and Simansky, 1997). Specifically, CP94253 reduces both meal size and meal duration without

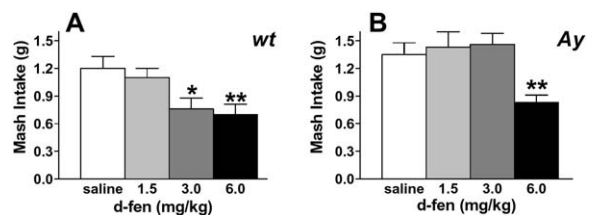


Figure 3. Response of Young, Lean Wild-Type Mice and *Ay* Littermates to the Classic Serotonergic Hypophagic Compound d-fen

(A) D-fen reduced 1 hr chow mash intake at the onset of the dark cycle in wild-type mice (n = 10, bw = 16–19 g, baseline mash intake = 0.97 ± 0.10 g) compared to saline treatment at a dose associated with satiety (3.0 mg/kg, i.p.) and a dose associated with the induction of behaviors that compete with feeding (6.0 mg/kg, i.p.).

(B) In contrast, 1 hr chow mash intake was not affected in *Ay* littermates (n = 10, bw = 16–20 g, baseline mash intake = 1.05 ± 0.12 g) treated with any dose of d-fen except that which is associated with the induction of behaviors that disrupt normal feeding patterns (6 mg/kg, i.p.). **p < 0.01, *p < 0.05 (compared to saline treatment). Data are expressed as mean ± SEM.

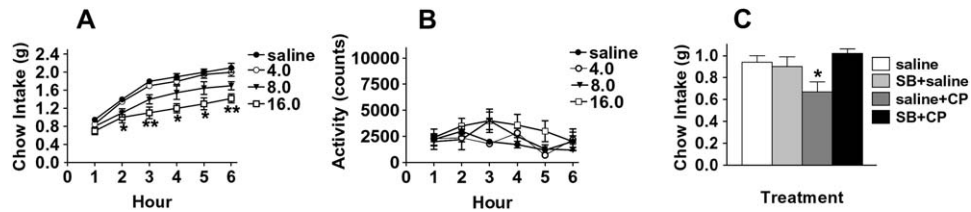


Figure 4. Hypophagic Effects of 5-HT_{1B}R Agonist CP94253 Are Independent of Alterations in Active Behavior and Are Mediated via Action at 5-HT_{1B}Rs

(A) Selective 5-HT_{1B}R agonist CP94253 (4.0, 8.0, 16.0 mg/kg, i.p.) dose-dependently reduced 6 hr dark cycle powdered chow intake in adult male C57BL/6 mice ($n = 16$, $bw = 20\text{--}26$ g, baseline 6 hr chow intake = 2.09 ± 0.4 g) assessed in Comprehensive Lab Animal Monitoring System (CLAMS) chambers. Post hoc analyses revealed that 8.0 mg/kg and 16.0 mg/kg significantly reduced food intake compared to saline treatment. (B) CP94253-induced hypophagia was independent of alterations in locomotor activity (baseline 6 hr activity = 2437 ± 633 counts/hr), which was concomitantly collected in the CLAMS chambers. (C) Hypophagia elicited by CP (CP94253; 8.0 mg/kg, i.p.) was abolished by pretreatment with the 5-HT_{1B}R antagonist SB (SB224289; 2.5 mg/kg, s.c.) in adult male 129/Sv-ter mice ($n = 9$, $bw = 21\text{--}26$ g) tested in the homecage following 18 hr food deprivation. Post hoc analyses demonstrated that CP94253 significantly reduced 1 hr chow pellet intake compared to saline treatment and that this effect was reversed by SB22489 pretreatment. ** $p < 0.01$, * $p < 0.05$ (compared to saline treatment). Data are expressed as mean \pm SEM.

altering oral motor efficiency compared to saline treatment in rats (Lee and Simansky, 1997). As a first step, we sought to confirm that CP94253 (4.0, 8.0, 16.0 mg/kg, i.p.) does not produce generalized effects on active/inactive behaviors in our hands. Male C57BL/6 mice ($n = 16$) were assessed during the first 6 hr of the dark cycle in comprehensive laboratory animal monitoring chambers, which concomitantly measure food intake and locomotor/horizontal activity. CP94253 (8.0, 16.0 mg/kg, i.p.) specifically reduced 6 hr powdered chow intake compared to saline [$F(5,15) = 2.10$, $p < 0.05$; Figure 4A] without significantly altering normal dark-cycle behavioral activity (ANOVA n.s.; Figure 4B).

We confirmed that CP94253-induced hypophagia was dependent on 5-HT_{1B}R stimulation by pretreating mice with the 5-HT_{1B}R antagonist SB224289 (K_i 5-HT_{1B}R = 6.3 nM and >100-fold greater affinity over other 5-HT₁Rs, 5-HT₂Rs, 5-HT₄R, 5-HT₆R, and 5-HT₇R; Selkirk et al., 1998). When administered alone, SB224289 (2.5 mg/kg, s.c.) did not significantly alter 1 hr chow pellet intake (Figure 4C). However, pretreatment with SB224289 abolished the hypophagic effect of 8.0 mg/kg CP94253 [$F(3, 24) = 4.02$, $p < 0.05$, post hoc saline + CP94253 versus SB224289 + CP94253; Figure 4C]. Together, these baseline studies confirm that CP94253 selectively decreases food intake via action at 5-HT_{1B}Rs, data which are in accord with previous findings (Halford and Blundell, 1996; Lee and Simansky, 1997; Lee et al., 2002).

To examine the importance of downstream MCRs in the hypophagic effect of 5-HT acting at 5-HT_{1B}Rs, we compared the response to CP94253 in three groups of weight-matched mice; Ay mice, *ob/ob* mice bearing a mutation in the leptin gene, and wild-type littermates ($n = 8$ per genotype). Consistent with that shown above, CP94253 (8.0, 16.0 mg/kg, i.p.) significantly reduced 6 hr chow mash intake in young wild-type [$F(2,14) = 6.68$, $p < 0.01$; Figure 5A] and *ob/ob* control mice [$F(2,14) = 6.97$, $p < 0.01$; Figure 5B], while, in contrast, the same doses of CP94253 did not alter food intake in Ay mice (ANOVA n.s.; Figure 5C). We next assessed the effect of CP94253 in older obese weight-matched mice with and without genetic alterations in melanocortin circuitry ($n = 7\text{--}8$ per genotype). Similar to data presented in mice in the young, nonobese state, CP94253 (8.0, 16.0 mg/kg, i.p.)

significantly reduced 6 hr consumption of 58% high-fat diet (HFD) in dietary-induced obese (DIO) mice [$F(2,14) = 6.68$, $p < 0.01$; Figure 5D] and *ob/ob* control mice [$F(2,14) = 6.14$, $p < 0.05$; Figure 5E], but did not affect food intake in Ay mice (ANOVA n.s.; Figure 5F). These findings demonstrate that the selective 5-HT_{1B}R agonist CP94253 requires downstream activation of MCRs to promote hypophagia in both the lean and obese state.

Mc4rs Are Downstream Targets of Selective 5-HT_{1B}R Agonist

We refined our model by hypothesizing that intact Mc4rs are a necessary downstream component of energy balance pathways engaged by 5-HT. To investigate this, we examined the efficacy of satiety-inducing doses of selective 5-HT_{1B}R agonist CP94253 (8.0 mg/kg, i.p.) and the 5-HT indirect agonist d-fen (3.0 mg/kg, i.p.) on chow pellet intake in strains of traditional *Mc4r* knockout (KO) mice (Huszar et al., 1997), *Mc3r* KO mice (Butler et al., 2000), and wild-type littermates 6 hr following the onset of the dark cycle ($n = 10\text{--}12$ per genotype). Consistent with that presented above, CP94253 significantly reduced food intake compared to saline in wild-type mice [$t(11) = 5.0$, $p < 0.001$; Figure 6A]. Supporting a role for the Mc4rs in this effect, *Mc3r* KO mice displayed a similar level of hypophagia in response to CP94253 [$t(11) = 6.5$, $p < 0.001$; Figure 6B] as wild-type littermates, while, in contrast, *Mc4r* KO mice were insensitive to the effects of this compound (t test n.s.; Figure 6C). We further explored the role of Mc4rs in 5-HT-induced satiety by investigating whether *Mc4r* KO mice were responsive to a more general 5-HT probe, the classic anorectic d-fen. Virtually identical data were obtained with satiety-associated doses of d-fen and the selective 5-HT_{1B}R agonist CP94253. Specifically, d-fen significantly decreased food intake compared to saline treatment in both wild-type mice [$t(11) = 5.7$, $p < 0.001$; Figure 6D] and *Mc3r* KO mice [$t(11) = 9.5$, $p < 0.001$; Figure 6E], but did not alter feeding in *Mc4r* KO mice (t test n.s.; Figure 6F).

To further clarify that activation of the Mc4rs is a primary mechanism through which 5-HT, via 5-HT_{1B}Rs, affects feeding behavior, we examined the hypophagic

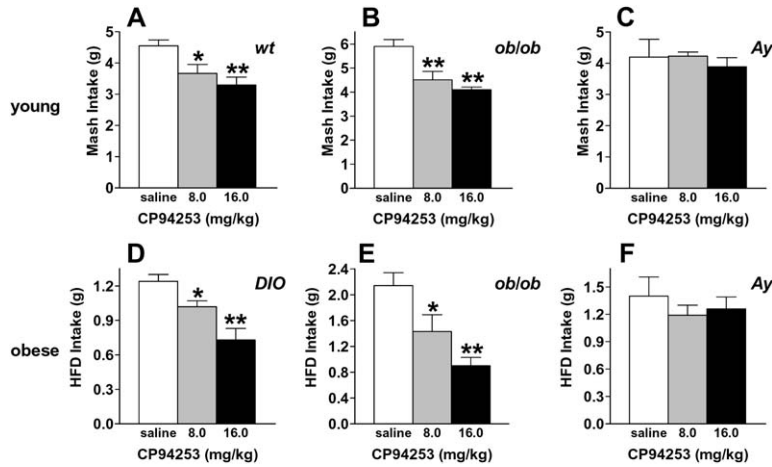


Figure 5. CP94253-Induced Hypophagia Requires Melanocortin Signaling

Selective 5-HT_{1B}R agonist CP94253 (8.0 and 16.0 mg/kg) significantly reduced 6 hr dark cycle chow mash intake in young lean (A) wild-type littermate (n = 8, bw = 18–23 g, baseline mash intake = 5.0 ± 0.54 g) and (B) age- and weight-matched *ob/ob* control mice (n = 8, bw = 18–22 g, baseline mash intake = 6.2 ± 0.43 g), but was not effective in altering food intake in (C) *Ay* mice (n = 8, bw = 16–23 g, baseline mash intake = 4.3 ± 0.59 g). Similarly, CP94253 (8.0 and 16.0 mg/kg) significantly reduced 6 hr dark cycle high-fat diet intake (HFD) in murine models of obesity (D) DIO (n = 8, bw = 30–38 g, baseline HFD intake = 1.4 ± 0.37 g) and (E) *ob/ob* mice (n = 7, bw = 40–44 g, baseline HFD intake = 2.5 ± 0.42 g), but did not affect feeding behavior in (F) *Ay* mice (n = 7, bw = 30–35 g, baseline HFD = 1.5 ± 0.33 g). DIO mice were littermates of *Ay* and *ob/ob* mice maintained on the HFD postweaning. **p < 0.01, *p < 0.05 (compared to saline treatment). Data are expressed as mean ± SEM.

efficacy of CP94253 and d-fen in another independently generated *Mc4r* null strain. We created this *Mc4r* null allele by inserting a transcriptional blocker (*loxTB*) sequence 5' of the *Mc4r* coding sequence (Balthasar et al., 2005). Mirroring data obtained with *Ay* mice and *Mc4r* KOs, older obese *loxTB Mc4r* mice were insensitive to hypophagic effects of CP94253 (8.0 mg/kg, i.p.) on 6 hr chow pellet intake [wild-type t(7) = 2.91, p < 0.05; *loxTB Mc4r* t test, n.s.; Figures 7A and 7B]. We next investigated whether results obtained in young lean *Ay* and *Mc4r* KO mice treated with d-fen would be mimicked in young lean *loxTB Mc4r* mice. Specifically, wild-type littermate and weight- and age-matched *loxTB Mc4r* null mice were treated with saline or d-fen (3.0 mg/kg i.p.), and subsequent intake of chow mash was measured for the next hour at the onset of the dark cycle (n = 8 per genotype). Like other mice with *Mc4r* disruption, *loxTB Mc4r* null mice did not respond to the hypophagic effect d-fen, whereas wild-type littermates significantly reduced food intake in response to

d-fen [wild-type t(7) = 2.82, p < 0.05; *loxTB Mc4r* t test, n.s.; Figures 7C and 7D].

The consistent finding that 5-HT agonist-induced hypophagia is blocked in mice with disrupted *Mc4r* function, whether *Ay*, *Mc4r* KO, or *loxTB Mc4r*, in either the lean or obese state, and when presented with palatable chow mash (Figures 3A, 3B, 5A–5C, 7C, and 7D), standard chow pellet (Figures 6A–6F, 7A, and 7B), or high-fat (Figures 5D–5F) diet, ascertains that the *Mc4r* is a necessary component of 5-HT regulation of satiety. These data establish that *Mc4rs*, but not *Mc3rs*, are critical downstream targets in 5-HT satiety pathways.

Discussion

Despite the established clinical utility of 5-HT-derived drugs in the induction of weight loss, the responsible mechanisms have remained obscure. We present evidence from a range of neuroanatomical, electrophysiological, transgenic, and behavioral studies that the central

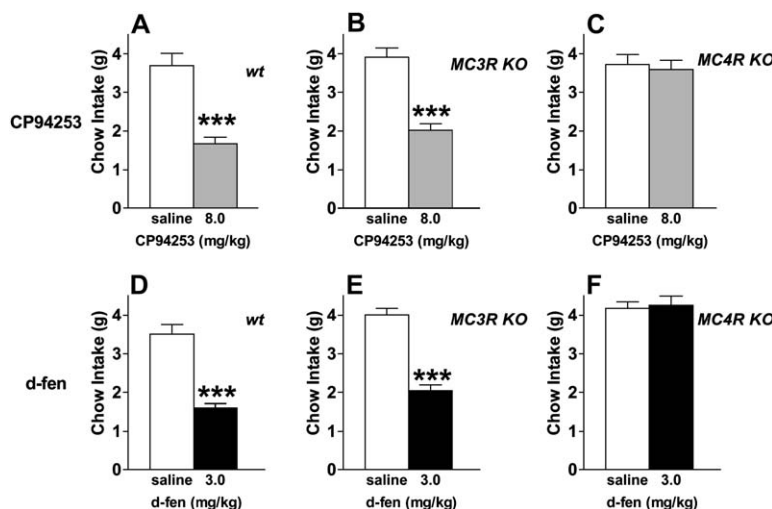


Figure 6. 5-HT Compounds Require *Mc4rs*, but Not *Mc3rs*, to Reduce Food Intake

Selective 5-HT_{1B}R agonist CP94253 (8.0 mg/kg, i.p.) significantly reduced 6 hr dark cycle chow pellet intake in young lean (A) wild-type (n = 12, bw = 20–22 g, baseline chow intake = 3.3 ± 0.17 g) and (B) *Mc3r* KO mice (n = 12, bw = 20–22 g, baseline chow intake = 3.3 ± 0.33 g), but did not alter food intake in (C) *Mc4r* KO littermates (n = 12, bw = 20–22 g, baseline chow intake = 3.7 ± 0.14 g). Similar results were obtained following d-fen (3.0 mg/kg). D-fen significantly reduced 6 hr dark cycle chow pellet intake in (D) wild-type and (E) *Mc3r* KO mice, but had no effect on food intake in (F) *Mc4r* KO littermates. ***p < 0.001 (compared to saline treatment). Data are expressed as mean ± SEM.

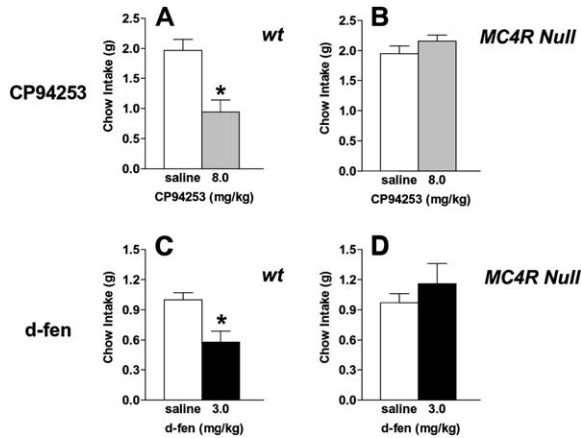


Figure 7. 5-HT Compounds Require Mc4rs to Reduce Food Intake
Selective 5-HT_{1B}R agonist CP94253 (8.0 mg/kg, i.p.) significantly reduced 6 hr dark cycle chow pellet intake in (A) wild-type mice (n = 8, bw = 26–31 g), but did not alter food intake in (B) obese *LoxTB Mc4r* littermates (n = 8, bw = 32–53 g). Similarly, d-fen (3.0 mg/kg) significantly reduced 60 min dark cycle chow mash intake in young lean (C) wild-type mice (n = 8, bw = 17–19 g), but had no effect on food intake in (D) *LoxTB Mc4r* littermates (n = 8, bw = 17–19 g). *p < 0.05 (compared to saline treatment). Data are expressed as mean ± SEM.

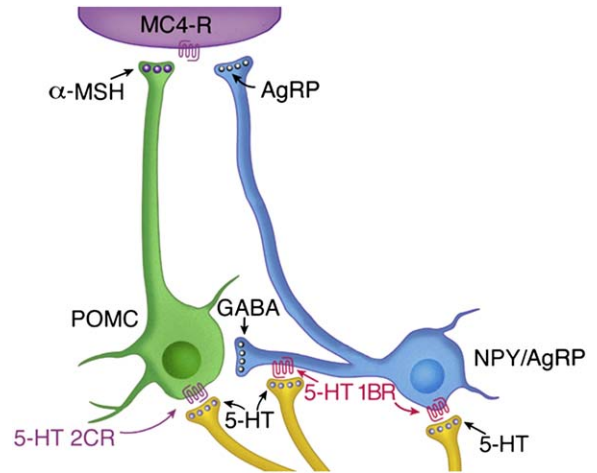


Figure 8. Schematic Diagram of Proposed 5-HT Sites of Action on Melanocortin Pathways
5-HT hyperpolarizes and inhibits AgRP neurons and decreases an inhibitory drive onto POMC cells by activation of 5-HT_{1B}Rs. 5-HT also activates POMC neurons via activation of 5-HT_{2C}Rs. This leads to reciprocal increases in α-MSH release and decreases in AgRP release at Mc4r in target sites.

melanocortin system is the key site of action of 5HT in the stimulation of hypophagia. We demonstrate that 5-HT, via 5-HT_{1B}Rs, both inhibits AgRP neuronal activity and reduces inhibitory postsynaptic currents onto POMC neurons. Complementing these data, we recently reported that 5-HT and 5-HT_{2C}R agonists stimulate POMC neurons (Heisler et al., 2002). The data presented here show that 5-HT differentially regulates melanocortin agonist- and antagonist-containing neurons and that downstream activation of Mc4rs is a primary mechanism through which 5-HT affects food intake. Figure 8 illustrates a proposed model of a mechanism through which 5-HT regulates energy balance via melanocortin pathways.

5-HT is a biogenic amine that is derived from the essential dietary amino acid tryptophan. Therefore, the dynamic interplay between nutritional intake and synthesis of 5-HT indicates that 5-HT, like other adiposity and metabolic cues, is inextricably linked to energy intake (Fernstrom and Wurtman, 1972). However, 5-HT also affects many other instinctual drives and behaviors that may interfere with feeding. It is therefore important to distinguish whether 5-HT compounds reduce food intake specifically by promoting satiety. For example, early pharmacological studies indicated that compounds such as d-fen and mCPP (a high-affinity 5-HT_{2C/1B} agonist) at lower concentrations specifically advanced satiety, but at higher concentrations, enhanced resting and by consequence suppressed active behaviors like feeding. As more selective 5-HTR compounds have become available, such as the 5-HT_{1B}R agonist CP94253, behavioral profiles more consistent with satiety at a range of doses have been found. Here we report that melanocortin pathways are a downstream target of d-fen and CP94253 at concentrations previously demonstrated to advance satiety.

Studies of targeted deletion of specific 5-HTRs indicate that 5-HT_{1B}Rs and 5-HT_{2C}Rs are the most critically involved 5-HTRs in the modulation of energy balance

(Lucas et al., 1998; Tecott et al., 1995). Specifically, deletion of either the 5-HT_{1B}R or 5-HT_{2C}R gene promotes enhanced body weight and attenuates responses to classic anorectic 5-HT compounds like d-fen (Bouwknicht et al., 2001; Lucas et al., 1998; Tecott et al., 1995). Here we investigated the mechanism through which 5-HT_{1B}R activation affects ingestive behavior. We demonstrated that 5-HT fibers make axo-somatic contacts with GFP-labeled NPY/AgRP neurons in the ARC and that a subpopulation of GFP-IR neurons expressed 5-HT_{1B}Rs. It is important to note that an accurate determination of the degree of coexpression is difficult to obtain as a result of the technological limitations frequently encountered with dual-labeling with ³⁵S-labeled 5-HTR riboprobe and IHC. However, it is clear that a subpopulation of ARC NPY/AgRP neurons coexpress 5-HT_{1B}R mRNA. We used an electrophysiological approach to investigate the functional relevance of these anatomical findings. Both 5-HT and 5-HT_{1B}R agonists hyperpolarized GFP-NPY neurons, effects that could be blocked by coapplication with a selective 5-HT_{1B}R antagonist. These data suggest that NPY/AgRP neurons are 5-HT responsive, via action at 5-HT_{1B}Rs.

5-HT terminals also make synaptic contacts with POMC neurons and stimulate these cells. We recently reported that 5-HT_{2C}Rs were coexpressed with POMC neurons and that 5-HT_{2C}R agonists dose-dependently depolarized POMC neurons (Heisler et al., 2002). Here we show that 5-HT fibers make additional axo-axonal contacts with NPY/AgRP terminals. Some NPY/AgRP terminals are GABAergic and make contacts with nearby POMC neurons, affecting POMC neuronal activity (Cowley et al., 2001; Roseberry et al., 2004). 5-HT_{1B}R agonists, like CP93129, have been demonstrated to reduce GABA release, an effect that is inhibited by 5-HT_{1B}R antagonist pretreatment (Chadha et al., 2000). We report that 5-HT and selective 5-HT_{1B}R agonists, like CP93129, significantly and consistently reduced

inhibitory postsynaptic currents onto POMC neurons. This reciprocal action on inhibitory and excitatory inputs into melanocortin neurons is reminiscent of that established for peripheral signals, such as leptin and ghrelin (Cowley et al., 2001; Roseberry et al., 2004).

To investigate whether regulation of melanocortin circuitry is critical to the effects of 5-HT on satiety, we examined the anorectic efficacy of 5-HT compounds in rodents with melanocortin receptor blockade. We recently reported that pretreatment with the Mc3/Mc4r antagonist SHU9119 attenuated the anorectic efficacy of the antiobesity compound d-fen (Heisler et al., 2002). Here we show that *Mc3r* KO mice treated with anorectic doses of d-fen and the 5-HT_{1B}R agonist CP94253 responded similarly to wild-type littermates, suggesting that Mc3rs are unlikely to be a downstream target of 5-HT-induced hypophagia. In contrast, the anorectic effect of both d-fen and CP94253 was abolished in *Ay*, *Mc4r* KO mice, and loxTB *Mc4r* null mice, strongly indicating that a primary mechanism of 5-HT-induced satiety is via action at downstream Mc4rs.

Here we present data in support of 5-HT regulation of activity of ARC neurons expressing the endogenous Mc4r antagonist AgRP and agonist α -MSH. However, the ARC is likely not the only site of 5-HT-melanocortin circuitry integration. Clear support for a brainstem locus of 5-HT hypophagic action has been provided by researchers such as Simansky and colleagues (Lee et al., 1998) and Grill and colleagues (Grill et al., 1997). For example, infusion of CP93129 into the lateral parabrachial nucleus (IPBN) dose-dependently reduced food intake (Lee et al., 1998). The IPBN is a key site involved in autonomic regulation, and we recently reported Mc4r expression in this region (Kishi et al., 2003; Liu et al., 2003). It is possible that 5-HT may make axo-axonal contacts with POMC and AgRP terminals arising from the ARC (or other inhibitory inputs) that form synaptic connections with Mc4r-expressing cells in sites such as the IPBN. 5-HT activation of 5-HT_{1B}R heteroreceptors expressed on these terminals may reduce inhibitory postsynaptic currents onto Mc4r-expressing neurons. This potential of 5-HT_{1B}R-Mc4r interaction outside of the ARC warrants investigation.

It is also important to note that other hypothalamic pathways are affected within our model. Specifically, if 5-HT affects POMC and AgRP neuronal activity, then the release of neuropeptides coexpressed in these neurons, such as cocaine and amphetamine-regulated transcript (CART) and NPY, respectively, should also be affected. Both CART and NPY alter food intake, and affecting the release of these neuropeptides may augment, interfere with, or have no effect on the results obtained with 5-HT agonists (Kristensen et al., 1998; Lambert et al., 1998). It is therefore striking that blockade of a single downstream target, the Mc4rs, is sufficient to render ineffective the 30%–50% reduction of food intake produced by classic 5-HTR agonists. These data were consistently observed, in both lean and obese mice presented with various diets. We conclude that reciprocal regulation of upstream hypothalamic melanocortin agonist- and antagonist-containing neurons and subsequent downstream activation of Mc4rs underlies the food-reducing properties of centrally derived classic appetite-regulating neurotransmitter 5-HT.

Experimental Procedures

Subjects

All mice were individually housed (except transgenic mice expressing green fluorescent protein, which were group housed) with food and water available ad libitum in a light- (12 hr on/12 hr off) and temperature-controlled environment (21.5°C–22.5°C). Adult male transgenic mice expressing GFP specifically in NPY (Cowley et al., 2003; Pinto et al., 2004; Roseberry et al., 2004) or POMC neurons (Cowley et al., 2001) were used for the electrophysiology experiments. Adult male NPY-GFP mice were used for the neurohistochemical analysis.

In feeding studies, young mice (5–8 weeks old) were weight-matched with littermates. Older obese mice (3–5 months old) were weight-matched with other murine models of obesity, such as dietary-induced obese mice (wild-type littermates of *Ay* and *ob/ob* mice, Jackson Laboratories) maintained on a 58% fat diet post-weaning (Research Diets) and *ob/ob* mice (B6.V-*Lep^{ob}*/J, Jackson Laboratories). Mice with disrupted melanocortin function were male *Ay* mice (B6.Cg-*A^y*/J, Jackson Laboratories), *Mc4r* KO (Huszar et al., 1997), loxTB *Mc4r* null mice (Balthasar et al., 2005), and *Mc3r* KO mice (Butler et al., 2000). All mice were on a C57BL/6 background, except loxTB *Mc4r* mice, which were on a mixed 129Sv and C57BL/6 background. Additional control wild-type feeding studies were performed in male 129/Sv-ter mice (University of Sussex colony).

Neurohistochemical Analysis

Tissue Preparation and Histology

Brain tissue was collected from adult male C57BL/6 and heterozygous NPY-GFP mice. Under deep anesthesia (350 mg/kg chloral hydrate, i.p.), mice were perfused transcardially with diethyl pyrocarbonate (DEPC)-treated 0.9% saline followed by 10% neutral buffered formalin or 4% paraformaldehyde. Brains were removed, immersed in the same fixative for 4 hr, and then in 20% sucrose in DEPC-treated phosphate-buffered saline (PBS pH 7.0) for 18–36 hr at 4°C. Brains were sectioned coronally on a freezing sliding microtome at 25 μ m (in situ hybridization histochemistry) or on a vibratome at 60 μ m (light and fluorescence microscopy).

Single-Label In Situ Hybridization Histochemistry

Visualization of 5-HT_{1B}R mRNA in the mouse brain ($n = 5$) was achieved with ISHH using similar methods to those previously described (Elias et al., 1999; Liu et al., 2003). A 5-HT_{1B}R riboprobe was generated using a 199-nt segment of the 3'-untranslated region of rat 5-HT_{1B}R as template. Plasmids were linearized by digestion with NotI (antisense) or Sall (sense). The riboprobe was subjected to in vitro transcription using a T3 polymerase (Ambion) in the presence of ³⁵S-labeled UTP in accordance with the manufacturer's protocols. The ³⁵S-labeled 5-HT_{1B}R cRNA probe was diluted to 10⁶ cpm/ml in a hybridization solution (Elias et al., 1999; Liu et al., 2003). Free-floating ISSH was performed using standard methods reported by our laboratory (Liu et al., 2003) in brain tissue from C57BL/6 mice ($n = 4$). Tissue was then mounted onto Superfrost slides, dehydrated in graded concentrations of ethanol, air-dried, and dipped in NTB2 photographic emulsion (Kodak). Slides were stored for 4 weeks at 4°C and then developed with D-19 Developer and Fixer (Kodak). Controls for specificity were performed by (1) hybridization following tissue pretreatment with RNase, (2) hybridization with the sense 5-HT_{1B}R riboprobe, and (3) comparing distribution of hybridization signal with published rodent 5-HT_{1B}R mRNA.

Dual-Label ISHH and Immunohistochemistry

Concurrent visualization of GFP and 5-HT_{1B}R mRNA or AgRP mRNA was performed by combining ISHH and IHC, using methods previously reported (Liu et al., 2003). Briefly, free-floating brain sections of NPY-GFP mice ($n = 3$ –4) were processed for ISHH as previously described (Liu et al., 2003) using ³⁵S-labeled 5-HT_{1B}R or ³⁵S-labeled AgRP riboprobes. While tissue was still free-floating, IHC was then performed to identify GFP-producing brain sites. Specifically, tissue was rinsed in 0.3% hydrogen peroxide (Sigma) in PBS, blocked in 3% normal donkey serum (Jackson ImmunoResearch Laboratories Inc.) in 0.25% Triton X-100 in PBS (PBT), incubated in a GFP rabbit primary antiserum (Molecular Probes, 1:20,000) in PBT, bathed with a biotinylated donkey anti-rabbit IgG (Jackson ImmunoResearch Laboratories Inc., 1:1000) secondary antibody in PBT, immersed in a solution of avidin-biotin complex (Vectastain Elite ABC

Kit; Vector Laboratories, 1:500) in PBS, and finally rinsed in a solution of 0.04% DAB (Sigma) and 0.01% hydrogen peroxide in PBS. Brain sections were then mounted onto Superfrost slides (Fisher Scientific), dehydrated, delipidated, air-dried, and dipped in NTB2 photographic emulsion (Kodak). Slides were stored in light-tight boxes at 4°C for 10 days (³⁵S-labeled AgRP) or 4 weeks (³⁵S-labeled 5-HT_{1B}R) and then developed with D-19 Developer and Fixer (Kodak). Determination of cells expressing both GFP-IR and ³⁵S-labeled AgRP or ³⁵S-labeled 5-HT_{1B}R was performed using criteria previously described (Elias et al., 1999; Liu et al., 2003). Briefly, clusters of grains (the hybridization signal) more than 3-fold background, overlying and conforming to the shape of a cell containing the GFP-IR signal, were considered a double-labeled cell. Adjacent series of sections were stained with thionin for the identification of nuclear boundaries. Photographs and schematic images were produced using a Zeiss Axioskop 2 mot plus with an interface with a Pentium III computer. Schematic Images were drawn using Canvas software.

Dual-IHC

Dual-IHC was performed to examine 5-HT inputs onto GFP-IR cell bodies and processes. To visualize dual-fluorescence imaging of 5-HT and GFP, IHC was performed as previously described (Liu et al., 2003; Pinto et al., 2004). Briefly, tissue from NPY-GFP mice (n = 3) was incubated with primary rabbit antiserum for 5-HT (Immunostar Inc., 1:5000) for 24 hr. A secondary anti-rabbit IgG labeled with Alexa Fluor 594 (Molecular Probes) was then applied, and a red fluorescent reaction product was obtained. After labeling for 5-HT, tissue was processed for GFP-IR. Tissue was incubated in mouse anti-GFP antiserum (Molecular Probes, 1:1000) for 24 hr at 4°C and then immersed in solution containing a secondary antibody (horse anti-mouse IgG conjugated with FITC diluted 1:50 in PBS Dako) for 2 hr. A green reaction product was obtained. Controls for specificity were performed by incubating sections in antisera that had been preadsorbed with the specific antigen (50 µg/ml of diluted antisera) and by omitting the incubation with the primary antisera step. Sections were mounted onto slides, ethanol-dehydrated, cleared in xylenes, and coverslipped with Vectashield mounting medium (Vector Labs). The dual fluorescence was assessed using fluorescence filters on a Zeiss Axiostar microscope equipped with an Axioplan 2 color camera. Putative contacts were detected under 100× magnification. Images were captured using a computer interface with the Zeiss Axiostar microscope and were displayed in panels using Photoshop software.

Electron Microscopic Immunocytochemistry

To examine light and electron microscopic analyses of 5-HT inputs onto ARC NPY/AgRP neurons, we combined pre- and postembedding immunolabeling of GFP and 5-HT (postembedding labeling of large core vesicles with 5 nm gold-conjugated secondary antisera) to investigate the ultrastructural relationship between GFP and 5-HT.

First, tissue was processed for IHC in a similar manner to that described above. Specifically, brain tissue from NPY-GFP mice (n = 5) was blocked in 3% normal donkey serum (Jackson ImmunoResearch Laboratories Inc.) in PBS for 1 hr. Next, tissue was incubated in a 5-HT rabbit primary antiserum (Immunostar, 1:25,000) in PBS for 12–18 hr. Sections were rinsed in PBS and then immersed in a biotinylated donkey anti-rabbit IgG (Jackson ImmunoResearch Laboratories Inc., 1:1000) secondary antibody for 1 hr. Tissue was rinsed in PBS and then incubated in a solution of ABC (Vectastain Elite ABC Kit; Vector Laboratories, 1:500) dissolved in PBS for 1 hr. Visualization of 5-HT was achieved using a nickel-DAB reaction (15 mg of DAB, 0.12 mg of glucose oxidase, 12 mg of ammonium chloride, 600 µl of 0.05M nickel ammonium sulfate, and 600 µl of 10% β-D-glucose in 30 ml of PBS) for 10–30 min, resulting in a dark blue-black reaction product. After several rinses in PBS, the sections were further incubated in mouse anti-GFP antiserum (Molecular Probes, 1:1000) for 24 hr at 4°C and then immersed in a secondary antibody (horse anti-mouse IgG diluted 1:50 in PBS, Dako) for 2 hr. Finally, tissue was incubated in rabbit peroxidase-anti-peroxidase (PAP; 1:100 in PBS, Dako) for 2 hr. Between each incubation step, the sections were rinsed (four times for 10 min each) in PBS. The tissue-bound peroxidase was visualized by a light brown DAB reaction. The colors of the two reaction products were easily distinguishable, and in single-stained material in which one of the primaries was omitted, only one color was seen. After immunostaining, the sections were thoroughly rinsed in PBS and processed for correlated electron micros-

copy. After visualization of tissue antigens, sections were wet-mounted in PBS and examined under the light microscope. Color photographs of GFP-IR NPY/AgRP cells contacted by putative 5-HT-immunoreactive axon terminals were captured using computer interface with the Zeiss Axiostar microscope. Sections were then osmicated, dehydrated, and embedded in araldite. Blocks were trimmed using the color picture of previously identified cells and boutons as a guide. Ribbons of serial ultrathin sections were collected on Formvar-coated single-slot grids and examined under the electron microscope. In a set of sections, after immunolabeling of GFP and embedding, ultrathin sections were further immunostained for 5-HT using the antisera described above in dilution of 1:25,000 and using 5 nm gold-conjugated secondary antisera. This procedure was carried out in accordance with our published protocol (Cowley et al., 2001, 2003; Pinto et al., 2004; Horvath and Gao, 2005).

Electrophysiology

Standard electrophysiological techniques were used, as previously published (Cowley et al., 2001; Heisler et al., 2002). Briefly, under iso-flurane anesthesia, male mice were rapidly decapitated and the brain was removed. Coronal hypothalamic slices containing the ARC were cut at 185 µm on a vibratome under ice-cold, gassed (95% O₂/5% CO₂) artificial cerebrospinal fluid (aCSF) of the following composition (mM): NaCl 126, KCl 2.5, MgCl₂ 1.2, CaCl₂ 2.4, NaH₂PO₄ 1.2, NaHCO₃ 21.4, glucose 11.1 (pH 7.4). Slices were maintained carbogenated at room temperature for 1 hr prior to recordings. Whole-cell patch-clamp recordings were obtained from POMC-GFP or NPY-GFP ARC neurons at 32°C ± 0.5°C. For membrane-potential recordings, current-clamp recordings were performed with patch pipettes (2–4 MΩ) filled with an intracellular solution of the following composition (mM): K gluconate 128, EGTA 1, KCl 10, MgCl₂ 1, CaCl₂ 0.3, (Mg) ATP 5, (Na)GTP 0.3, HEPES 10 (pH 7.3) (with NaOH), 290 mOsm. For inhibitory postsynaptic potential recordings, voltage-clamp recordings were performed with patch pipettes (2–4 MΩ) filled with a cesium-based intracellular solution of the following composition (mM): CsCl 140, MgCl₂ 5, (Mg) ATP 5, (Na)GTP 0.3, BAPTA 1, HEPES 10 (pH 7.3) (with CsOH), 290 mOsm. Because of the stochastic firing properties of arcuate NPY neurons, 10 min of baseline data were recorded for each arcuate neuron prior to drug application. Only stable cells were treated with drugs. Drugs were applied at the specified concentrations in the superfusion medium by gravity for approximately 4 min. Recordings were obtained by a Axopatch 200B patch-clamp amplifier and analyzed using pClamp 8.0 (Axon Instruments) and MiniAnalysis 5.0 (Synaptosoft, Inc.).

Feeding and Locomotor Studies

Food was removed and drug or vehicle was administered at 45 min prior to the onset of the dark cycle to ad libitum fed mice (n = 8–12 per genotype in each testing condition). Food was replaced at the onset of the dark cycle, and subsequent food intake and/or locomotor activity were recorded for the next 1–6 hr. A subset of male wild-type 129/Sv-ter mice (n = 9) were food deprived for 18 hr, received saline or 5-HT_{1B}R antagonist pretreatment, and 30 min later received 5-HT_{1B}R agonist treatment. Chow was then provided, and intake was measured for the next hour. All mice were provided with one of the following diets: chow pellets available in a hopper above the cage, high-fat paste diet (58% fat, Research Diets) provided in glass jars within the cage, chow mash diet (powdered Purina Rodent Chow and water at 1:1 concentration) provided in plastic jars within the cage, or powdered laboratory Purina Rodent Chow provided in the CLAMS apparatus described below. All studies were performed in the homecage, with the exception of those conducted in the CLAMS chambers. Each mouse was tested with both drug and saline, administered in a counterbalanced order, with a minimum of 3 days between the treatments.

Comprehensive Lab Animal Monitoring System

CLAMS (Columbus Instruments) chambers were used to assess the effect of CP94253 on acute food intake and locomotor activity. CLAMS chambers are plexiglass 1 l rectangular cages with a two-level photobeam array surround for locomotor activity determination. A spring-loaded grate covered powdered standard laboratory chow, such that as food is consumed, the grate is lowered. The feeder is attached to a balance and food intake is recorded in an

automated manner. All activity and feeding data are electronically collected and stored in a time-stamped data file. Mice were acclimated to the chambers prior to the start of the study, during which time food intake and body weight was monitored and compared to homecage conditions. Once stable feeding patterns were evident, mice underwent the experimental treatment.

Drugs

D-fenfluramine (Sigma), 5-HT (Sigma), CP94253 (Tocris Cookson, Vernalis Research Ltd, or kindly provided by Phoenix Pharmaceuticals), CP93129 (Tocris Cookson), and SB224289 (Vernalis Research Ltd or Tocris Cookson) were used. All drugs, except SB224289 (Vernalis Research Ltd) used in *in vivo* studies, were dissolved in 0.9% pyrogen-free saline and administered intraperitoneally (i.p.) in a volume of 10 μ l/g of body weight. SB224289 was initially dissolved in 20% of the final volume of PEG400, sonicated for 20 min, and made up to volume with 10% 2-hydroxypropyl- β -cyclodextrin (Fluka) in water, and administered subcutaneously (s.c.) in a volume of 4 μ l/g of body weight.

Data Analysis

Behavioral data were collected in a within-subjects design, such that each mouse acted as its own control. Prior to performing statistical tests, data were assessed for normality with Shapiro-Wilk's test using SPSS PC Advanced Statistics (v. 11.5) software. All data were normally distributed and were analyzed with either a one-sample t test (electrophysiology data), dependent t test (for saline and one drug dose behavioral comparisons), or repeated-measures analysis of variance (RM ANOVA), followed by Tukey's post hoc tests (for saline and more than one drug dose behavioral comparisons). For all analyses, significance was assigned at the $p \leq 0.05$ level.

Acknowledgments

We would like to thank Julie Ousteky, Ryan White, Vinsee Tang, and Chris Kenny for their invaluable assistance. Data presented in this paper were supported by the following L.K.H. (NIDDK DK065171, American Diabetes Association, and Boston Obesity Nutrition Research Center), N.B. (The Wellcome Trust, UK, ADA-EASD Transatlantic Fellowship, and Boston Obesity Nutrition Research Center), P.G.C. (BBSRC C505291), B.B.L. (NIDDK56116 and DK53301), A.A.B. (NIDDK DK068330 and American Diabetes Association), T.H. (NIDDK DK074386 and DK060711), J.K.E. (NIMH MH061583, NIDDK P01DK056116), and M.A.C. (NIH RR 00163, NIDDK, DK62202). M.A.C. and OHSU have a significant financial interest in Orexigen Therapeutics Inc., a company that may have a commercial interest in the results of this research and technology. This potential conflict of interest has been reviewed and managed by the OHSU Conflict of Interest in Research Committee and the Integrity Program Oversight Council.

Received: May 24, 2005

Revised: February 3, 2006

Accepted: June 6, 2006

Published: July 19, 2006

References

Ahima, R.S., Kelly, J., Elmquist, J.K., and Flier, J.S. (1999). Distinct physiological and neuronal responses to decreased leptin and mild hyperleptinemia. *Endocrinology* 140, 4923–4931.

Balthasar, N., Dalgaard, L.T., Lee, C.E., Yu, J., Funahashi, H., Williams, T., Ferreira, M., Tang, V., McGovern, R.A., Kenny, C.D., et al. (2005). Divergence of melanocortin pathways in the control of food intake and energy expenditure. *Cell* 123, 493–505.

Bonaventure, P., Voorn, P., Luyten, W.H., Jurzak, M., Schotte, A., and Leysen, J.E. (1998). Detailed mapping of serotonin 5-HT1B and 5-HT1D receptor messenger RNA and ligand binding sites in guinea-pig brain and trigeminal ganglion: clues for function. *Neuroscience* 82, 469–484.

Bouwknegt, J.A., van der Gugten, J., Hijzen, T.H., Maes, R.A., Hen, R., and Olivier, B. (2001). Male and female 5-HT(1B) receptor knock-

out mice have higher body weights than wildtypes. *Physiol. Behav.* 74, 507–516.

Breisch, S.T., Zemlan, F.P., and Hoebel, B.G. (1976). Hyperphagia and obesity following serotonin depletion by intraventricular p-chlorophenylalanine. *Science* 192, 382–385.

Broberger, C., De Lece, L., Sutcliffe, J.G., and Hokfelt, T. (1998). Hypocretin/orexin- and melanin-concentrating hormone-expressing cells form distinct populations in the rodent lateral hypothalamus: relationship to the neuropeptide Y and agouti gene-related protein systems. *J. Comp. Neurol.* 402, 460–474.

Bruinvels, A.T., Landwehrmeyer, B., Gustafson, E.L., Durkin, M.M., Mengod, G., Branchek, T.A., Hoyer, D., and Palacios, J.M. (1994). Localization of 5-HT1B, 5-HT1D alpha, 5-HT1E and 5-HT1F receptor messenger RNA in rodent and primate brain. *Neuropharmacology* 33, 367–386.

Butler, A.A., Kesterson, R.A., Khong, K., Cullen, M.J., Pelleymounter, M.A., Dekoning, J., Baetscher, M., and Cone, R.D. (2000). A unique metabolic syndrome causes obesity in the melanocortin-3 receptor-deficient mouse. *Endocrinology* 141, 3518–3521.

Chadha, A., Sur, C., Atack, J., and Duty, S. (2000). The 5HT(1B) receptor agonist, CP-93129, inhibits [(3)H]-GABA release from rat globus pallidus slices and reverses akinesia following intrapallidal injection in the reserpine-treated rat. *Br. J. Pharmacol.* 130, 1927–1932.

Cone, R.D. (2005). Anatomy and regulation of the central melanocortin system. *Nat. Neurosci.* 8, 571–578.

Cowley, M.A., Smart, J.L., Rubinstein, M., Cerdan, M.G., Diano, S., Horvath, T.L., Cone, R.D., and Low, M.J. (2001). Leptin activates anorexigenic POMC neurons through a neural network in the arcuate nucleus. *Nature* 411, 480–484.

Cowley, M.A., Smith, R.G., Diano, S., Tschop, M., Pronchuk, N., Grove, K.L., Strasburger, C.J., Bidlingmaier, M., Esterman, M., Heiman, M.L., et al. (2003). The distribution and mechanism of action of ghrelin in the CNS demonstrates a novel hypothalamic circuit regulating energy homeostasis. *Neuron* 37, 649–661.

Elias, C.F., Lee, C., Kelly, J., Aschkenasi, C., Ahima, R.S., Couceyro, P.R., Kuhar, M.J., Saper, C.B., and Elmquist, J.K. (1998). Leptin activates hypothalamic CART neurons projecting to the spinal cord. *Neuron* 21, 1375–1385.

Elias, C.F., Aschkenasi, C., Lee, C., Kelly, J., Ahima, R.S., Bjorbaek, C., Flier, J.S., Saper, C.B., and Elmquist, J.K. (1999). Leptin differentially regulates NPY and POMC neurons projecting to the lateral hypothalamic area. *Neuron* 23, 775–786.

Elmquist, J.K., Elias, C.F., and Saper, C.B. (1999). From lesions to leptin: hypothalamic control of food intake and body weight. *Neuron* 22, 221–232.

Fan, W., Dinulescu, D.M., Butler, A.A., Zhou, J., Marks, D.L., and Cone, R.D. (2000). The central melanocortin system can directly regulate serum insulin levels. *Endocrinology* 141, 3072–3079.

Farooqi, I.S., Yeo, G.S., Keogh, J.M., Aminian, S., Jebb, S.A., Butler, G., Cheetham, T., and O'Rahilly, S. (2000). Dominant and recessive inheritance of morbid obesity associated with melanocortin 4 receptor deficiency. *J. Clin. Invest.* 106, 271–279.

Fernstrom, J.D., and Wurtman, R.J. (1972). Brain serotonin content: physiological regulation by plasma neutral amino acids. *Science* 178, 414–416.

Garattini, S., Mennini, T., Bendotti, C., Invernizzi, R., and Samanin, R. (1986). Neurochemical mechanism of action of drugs which modify feeding via the serotonergic system. *Appetite Suppl.* 7, 15–38.

Goudie, A.J., Thornton, E.W., and Wheeler, T.J. (1976). Effects of Lilly 110140, a specific inhibitor of 5-hydroxytryptamine uptake, on food intake and on 5-hydroxytryptophan-induced anorexia. Evidence for serotonergic inhibition of feeding. *J. Pharm. Pharmacol.* 28, 318–320.

Grill, H.J., Donahey, J.C., King, L., and Kaplan, J.M. (1997). Contribution of caudal brainstem to d-fenfluramine anorexia. *Psychopharmacology (Berl.)* 130, 375–381.

Gropp, E., Shanabrough, M., Borok, E., Xu, A.W., Janoschek, R., Buch, T., Plum, L., Balthasar, N., Hampel, B., Waisman, A., et al.

- (2005). Agouti-related peptide-expressing neurons are mandatory for feeding. *Nat. Neurosci.* *8*, 1289–1291.
- Hahn, T.M., Breininger, J.F., Baskin, D.G., and Schwartz, M.W. (1998). Coexpression of AgRP and NPY in fasting-activated hypothalamic neurons. *Nat. Neurosci.* *1*, 271–272.
- Halford, J.C., and Blundell, J.E. (1996). The 5-HT_{1B} receptor agonist CP-94,253 reduces food intake and preserves the behavioural satiety sequence. *Physiol. Behav.* *60*, 933–939.
- Heisler, L.K., Cowley, M.A., Tecott, L.H., Fan, W., Low, M.J., Smart, J.L., Rubinstein, M., Tatro, J.B., Marcus, J.N., Holstege, H., et al. (2002). Activation of central melanocortin pathways by fenfluramine. *Science* *297*, 609–611.
- Horvath, T.L., and Gao, X.B. (2005). Input organization and plasticity of hypocretin neurons: possible clues to obesity's association with insomnia. *Cell Metab.* *1*, 279–286.
- Huszar, D., Lynch, C.A., Fairchild-Huntress, V., Dunmore, J.H., Fang, Q., Berkemeier, L.R., Gu, W., Kesterson, R.A., Boston, B.A., Cone, R.D., et al. (1997). Targeted disruption of the melanocortin-4 receptor results in obesity in mice. *Cell* *88*, 131–141.
- Kishi, T., Aschkenasi, C.J., Lee, C.E., Mountjoy, K.G., Saper, C.B., and Elmquist, J.K. (2003). Expression of melanocortin 4 receptor mRNA in the central nervous system of the rat. *J. Comp. Neurol.* *457*, 213–235.
- Koe, K.B., Nielsen, J.A., Macor, J.E., and Heym, J. (1992). Biochemical and behavioural studies of the 5-HT_{1B} receptor agonist, CP-94,253. *Drug Dev. Res.* *26*, 241–250.
- Kristensen, P., Judge, M.E., Thim, L., Ribel, U., Christjansen, K.N., Wulff, B.S., Clausen, J.T., Jensen, P.B., Madsen, O.D., Vrang, N., et al. (1998). Hypothalamic CART is a new anorectic peptide regulated by leptin. *Nature* *393*, 72–76.
- Lambert, P.D., Couceyro, P.R., McGirr, K.M., Dall Vechia, S.E., Smith, Y., and Kuhar, M.J. (1998). CART peptides in the central control of feeding and interactions with neuropeptide Y. *Synapse* *29*, 293–298.
- Lee, M.D., and Simansky, K.J. (1997). CP-94, 253: a selective serotonin_{1B} (5-HT_{1B}) agonist that promotes satiety. *Psychopharmacology (Berl.)* *131*, 264–270.
- Lee, M.D., Aloyo, V.J., Fluharty, S.J., and Simansky, K.J. (1998). Infusion of the serotonin_{1B} (5-HT_{1B}) agonist CP-93,129 into the parabrachial nucleus potently and selectively reduces food intake in rats. *Psychopharmacology (Berl.)* *136*, 304–307.
- Lee, M.D., Kennett, G.A., Dourish, C.T., and Clifton, P.G. (2002). 5-HT_{1B} receptors modulate components of satiety in the rat: behavioural and pharmacological analyses of the selective serotonin_{1B} agonist CP-94,253. *Psychopharmacology (Berl.)* *164*, 49–60.
- Lee, M.D., Somerville, E.M., Kennett, G.A., Dourish, C.T., and Clifton, P.G. (2004). Reduced hypophagic effects of d-fenfluramine and the 5-HT_{2C} receptor agonist mCPP in 5-HT_{1B} receptor knockout mice. *Psychopharmacology (Berl.)* *176*, 39–49.
- Liu, H., Kishi, T., Roseberry, A.G., Cai, X., Lee, C.E., Montez, J.M., Friedman, J.M., and Elmquist, J.K. (2003). Transgenic mice expressing green fluorescent protein under the control of the melanocortin-4 receptor promoter. *J. Neurosci.* *23*, 7143–7154.
- Lucas, J.J., Yamamoto, A., Searce-Levie, K., Saudou, F., and Hen, R. (1998). Absence of fenfluramine-induced anorexia and reduced c-Fos induction in the hypothalamus and central amygdaloid index of serotonin 1B receptor knock-out mice. *J. Neurosci.* *18*, 5537–5544.
- Luquet, S., Perez, F.A., Hnasko, T.S., and Palmiter, R.D. (2005). NPY/AgRP neurons are essential for feeding in adult mice but can be ablated in neonates. *Science* *310*, 683–685.
- Makarenko, I.G., Meguid, M.M., and Ugrumov, M.V. (2002). Distribution of serotonin 5-hydroxytryptamine 1B (5-HT_{1B}) receptors in the normal rat hypothalamus. *Neurosci. Lett.* *328*, 155–159.
- Mountjoy, K.G., Mortrud, M.T., Low, M.J., Simerly, R.B., and Cone, R.D. (1994). Localization of the melanocortin-4 receptor (MC4-R) in neuroendocrine and autonomic control circuits in the brain. *Mol. Endocrinol.* *8*, 1298–1308.
- Pinto, S., Roseberry, A.G., Liu, H., Diano, S., Shanabrough, M., Cai, X., Friedman, J.M., and Horvath, T.L. (2004). Rapid rewiring of arcuate nucleus feeding circuits by leptin. *Science* *304*, 110–115.
- Roseberry, A.G., Liu, H., Jackson, A.C., Cai, X., and Friedman, J.M. (2004). Neuropeptide Y-mediated inhibition of proopiomelanocortin neurons in the arcuate nucleus shows enhanced desensitization in ob/ob mice. *Neuron* *41*, 711–722.
- Samanin, R., Mennini, T., and Garattini, S. (1980). Evidence that it is possible to cause anorexia by increasing release and/or directly stimulating postsynaptic serotonin receptors in the brain. *Prog. Neuropsychopharmacol.* *4*, 363–369.
- Selkirk, J.V., Scott, C., Ho, M., Burton, M.J., Watson, J., Gaster, L.M., Collin, L., Jones, B.J., Middlemiss, D.N., and Price, G.W. (1998). SB-224289—a novel selective (human) 5-HT_{1B} receptor antagonist with negative intrinsic activity. *Br. J. Pharmacol.* *125*, 202–208.
- Stanford, I.M., and Lacey, M.G. (1996). Differential actions of serotonin, mediated by 5-HT_{1B} and 5-HT_{2C} receptors, on GABA-mediated synaptic input to rat substantia nigra pars reticulata neurons in vitro. *J. Neurosci.* *16*, 7566–7573.
- Tecott, L.H., Sun, L.M., Akana, S.F., Strack, A.M., Lowenstein, D.H., Dallman, M.F., and Julius, D. (1995). Eating disorder and epilepsy in mice lacking 5-HT_{2c} serotonin receptors. *Nature* *374*, 542–546.
- Vaisse, C., Clement, K., Guy-Grand, B., and Froguel, P. (1998). A frameshift mutation in human Mc4r is associated with a dominant form of obesity. *Nat. Genet.* *20*, 113–114.
- Vickers, S.P., Clifton, P.G., Dourish, C.T., and Tecott, L.H. (1999). Reduced satiating effect of d-fenfluramine in serotonin 5-HT_{2C} receptor mutant mice. *Psychopharmacology (Berl.)* *143*, 309–314.